Neuroendocrinology Letters Volume 45 No. 3 2024
ISSN: 0172-780X; ISSN-L: 0172-780X; Electronic/Online ISSN: 2354-4716
Web of Knowledge / Web of Science: Neuroendocrinol Lett
Pub Med / Medline: Neuro Endocrinol Lett

ORIGINAL ARTICLE

Protective effects and mechanisms of deer blood phospholipids (DBP) on zearalenone-induced oxidative damage in swine Sertoli cells.

Yile Sun[1,2,3*], Hongmei Gao[2*], Yiwei Wang[3], Guoshi Liu[3], Bingyuan Wang[2,3], Huansheng Han[1]

1 College of Animal Science and Technology, Heilongjiang Bayi Agricultural University, Daqing 163319, China.
2 Institute of Animal Sciences, Chinese Academy of Agricultural Sciences, Beijing 100193, China.
3 College of Animal Science and Technology, China Agricultural University, Beijing 100193, China.

*Yile Sun and Hongmei Gao are co-first authors.

Correspondence to: Bingyuan Wang, PhD
Institute of Animal Sciences, Chinese Academy of Agricultural Sciences, Beijing 100193, China and College of Animal Science and Technology, China Agricultural University, 100193, China
TEL: 010-62732735, E-MAIL: wangbingyuan@cau.edu.cn
Huansheng Han, PhD
College of Animal Science and Technology, Heilongjiang Bayi Agricultural University, Daqing 163319, China
TEL: 0459-6819195, E-MAIL: hanhuansheng@aliyun.com

Submitted: 2024-03-15 Accepted: 2024-04-06 Published online: 2024-07-28

Key words: **Deer blood phospholipids (DBP); Zearalenone (ZEA); swine; Sertoli cells (SCs); oxidative damage**

Neuroendocrinol Lett 2024; **45**(3):215–228 **PMID:** 39146567 NEL450324A06

Abstract

BACKGROUND: The swine Sertoli cells (SCs) are more vulnerable to the environmental insults than other species. We observed that zearalenone (ZEA), a prevalent food contaminant, caused SCs oxidative damage and inhibits their proliferation. Therefore, a naturally occurring antioxidant, i.e., the deer blood phospholipids (DBP) has been selected to test its potentially protective effects on SCs.
METHODS: Collect fresh samples of swine testicles, isolated, cultured and identified primary swine SCs. The ROS levels in SCs 24 h induced by different concentrations of ZEA were detected, and the oxidative damage model was established. After DBP was added to the SCs 24 h after the damage, the oxidative and antioxidant indexes were detected by ELISA kit. Finally, the protective mechanism of DBP was explained by RNA-seq.
RESULTS: The results showed that DBP effectively protected against the reproductive toxicity induced by ZEA. The protective effects of DBP were mainly mediated by its potent antioxidative capacity. DBP upregulated the activities of the endogenous antioxidant enzymes including CAT and GSH-PX and reduced intracellular ROS level and MDA. In addition, DBP also promoted the SCs proliferation. The transcriptome sequencing combined with DEGs, GO and KEGG analyses suggested that DBP treatment enriched various signaling pathways of potentially biological significance including MAPK and PI3K-Akt signaling pathways. Both pathways also promote the cell proliferation. EdU assay further confirmed the beneficial effects of DBP on SCs proliferation.

CONCLUSION: DBP will be considered as a suitable candidate to find its use in improvement of male swine reproductive activity.

Abbreviations:

SCs	- Sertoli cells
ZEA	- Zearalenone
DBP	- Deer blood phospholipids
ROS	- Reactive oxygen species
CAT	- Catalase
GSH-PX	- Glutathione peroxidase
RNA-seq	- RNA sequencing
MDA	- Malondialdehyde
GO	- Gene Ontology
KEGG	- Kyoto Encyclopedia of Genes and Genomes

INTRODUCTION

Swine is one of the most important livestock to provide meat and other nutritional products to humans' daily life. Our increased demanding for meat consumption requires researchers to continuously improve the breeding efficiency of swine. Many factors contribute to the swine breeding efficiency and the high quality of sperm is one of them (Mellagi *et al.* 2023). However, the sperm is vulnerable for oxidative stress. The excessive oxidative stress will lead to sperm abnormalities including oligospermia, necrospermia, and sperm deformities which significantly jeopardize the reproductive efficiency of the swine (Abah *et al.* 2023; Ayad *et al.* 2022; Nguyen *et al.* 2023; Sengupta *et al.* 2022). Regarding to the reproductive physiology, Sertoli cells (SCs) are the only somatic cells that compose the testicular cytoskeleton, establishing direct contact with spermatogenic cells. SCs form a blood-testis barrier that prevents harmful substances entering the spermatogenic epithelium. They also provide structural and functional support to maintain spermatogenic development (Cao *et al.* 2021). However, swine SCs are susceptible to the primary action of various toxicants and are particularly sensitive to environmental pollutes (Gao *et al.* 2015) such as zearalenone (ZEA).

ZEA, known as F-2 toxin, is a prevalent non-steroidal mycotoxin. Its metabolite shares a similar structure to the endogenous estrogen 17 β-estradiol in animals (Kuiper *et al.* 1998; Li *et al.* 2021), and it competitively binds to estrogen receptors in various tissues, including the ovary (Gajęcka *et al.* 2011), uterus (Yan *et al.* 2022b), mammary gland, penis, testes, epididymis, and prostate gland. This binding disrupts the endocrine function and triggers symptoms such as ovarian and uterine dilatation, decreased sperm count, and reduced serum testosterone concentration (Minervini *et al.* 2001; Zinedine *et al.* 2007). Studies have shown that the estrogen like effects occur in the orders of α-zearalenol > ZEA > β-zearalenol (Sforza *et al.* 2006). Since ZEA is metabolized to α-zearalenol in swine, this makes ZEA be more toxic in swine than other species (Sun *et al.* 2022).

In addition, ZEA causes mitochondrial damage in testicular interstitial cells and inhibits testosterone secretion (Li *et al.* 2014). The in vitro study showed that the addition of ZEA to swine seminal fluid resulted in reduced sperm fertilization (Tsakmakidis *et al.* 2006). Feeding male swine and mice with ZEA-containing feed significantly decreased sperm count and quality (Kiseleva *et al.* 2020). Feeding sows with ZEA also led to microscopic changes in reproductive organs, affecting oviduct and uterine function (Soffa *et al.* 2023). Furthermore, it severely affected the body condition and offspring development during pregnancy and lactation (Zhang *et al.* 2015). Several studies have confirmed oxidative damage induced by ZEA being a vital mechanism for its reproductive toxicity (Cimbalo *et al.* 2022; Qin *et al.* 2015). Therefore, identification of the reliable antioxidants is an effective strategy for mitigating the toxicity of ZEA on swine reproduction and to improve the swine breeding efficiency.

Deer blood extracts have remarkable therapeutic effect on bruises, rheumatism, and even have anti-aging activity (Sun *et al.* 2024; Wilson & Pauli 1983). Phospholipid of deer blood (DBP) was extracted by ultrasonic-assisted Folch method (Zhao & Xu 2010), and the phospholipid obtained by the modified method had a phosphorus content of 4.24%, which was consistent with the UV-VIS absorption spectrum of lecithin in dichloromethane. In vitro experiments have shown that DBP scavenged 2,2-Diphenyl-1-picrylhydrazyl radical (DPPH•) and hydroxyl radical (•OH) (He. 2022). In the in vivo study these bioactive phospholipids exhibited anti-inflammatory and immunomodulatory properties (Vicenova *et al.* 2014). Similarly, phospholipids extracted from egg yolk and soybean also reduced liver weight, liver triglyceride and MDA contents, and serum ALT, AST, TBA as well as CRP levels in rats fed high fructose, indicating hypolipidemia and anti-inflammatory effects (Yin *et al.* 2021). In ovariectomized rats orally administration of pilose antler blood at the dose of 4000 microl/kg daily for 10 weeks reduced osteoporosis by restoring bone mineral density in the lumbar spine and left femur (Yang *et al.* 2010). In RAW 264.7 cells, antler water extract treatment had an anti-inflammatory effect by reducing the production of pro-inflammatory cytokines, including tumor necrosis factor α (TNF-α) and interleukin-6 (IL-6) which were elevated by lipopolysaccharide (LPS) stimulation (Kuo *et al.* 2018). These findings suggest that the active phospholipids derived from deer blood displays antioxidant activity. However, as a novel and highly efficient antioxidant, its application in ZEA induced swine SCs oxidative damage has not been investigated.

In this study, we have aimed to establish a model of ZEA induced swine SCs oxidative damage to investigate whether DBP has protective effects. The examined parameters include cellular activity and morphology, tissue oxidative stress and antioxidant

levels. Additionally, transcriptome sequencing will be performed to identify the potential protective mechanism of DBP. The ultimate objective is to provide novel therapeutic and preventive strategies for safeguarding swine SCs against oxidative damage to improve the reproduction efficiency of swine.

MATERIALS & METHODS

Chemicals and agents

Zearalenone were purchased from Med Chem Express (Cat. NO.: HY-103447, Monmouth Junction, NJ, USA), and then dissolved in dimethyl sulfoxide (DMSO). The DBP was obtained by improving the classical method of lipid extraction, the Folch method, and coordinated ultrasonic extraction technology. purchased from the Laboratory of Biomaterials of Harbin Institute of Technology, the drug has applied for national invention patent, patent No.: CN 115043872A: The DBP is a light pink powder, dissolved in Duchenne phosphate cache solution (DPBS) (Guo *et al.*2022). After preparation, it is sealed in a container filled with nitrogen avoid expose to oxygen.

Collection of testicular tissue

This study was conducted in strict accordance with the recommendations of the Guide for the Animal Care and Use Committee of the Institute of Animal Sciences, Chinese Academy of Agricultural Sciences. The approved protocol number is IAS2021-6. Testes from 7-9 days old Bamin Black swine (crossed by Bakshire Black swine and Folk swine) were collected, which were then immersed in pre-cooled DPBS (Gibco, Cat. NO.: C14190500BT) supplemented with a 5-fold dilution of double antibiotics (Penicillin-Streptomycin, also known as PS, Gibco, Cat. NO.: 15140-122) before transportation back to the laboratory.

Histological observation of testis

Fresh testes were carefully cleaned using DPBS to remove connective tissues and incised leucorrhea. Tissue samples, measuring 1 mm^3, were subsequently soaked in testis fixative solution (Service bio, Cat. NO.: G1121) and processed to create paraffin sections. The samples were passed the processes of dehydration, clearing, wax embedding, section spreading, and baking, respectively in orders. The paraffin sections were then dewaxed, hydrotreated, subjected to HE staining for 30 min. Then the samples were dehydrated, cleared, and sealed with neutral resin to complete the HE stains process.

SCs Isolation and culture

The testes were soaked in pre-cooled 75% ethanol for 5 min, followed by three washes with DPBS containing 2×PS. Next, the cleaned testes were carefully transferred to a 6 cm dish, allowing for the removal of impurities such as the scrotum, sheath, blood vessels, and epididymis without causing damage to the tunica albuginea structure of the testes. During the process, a small amount of DPBS was added to keep the tissue moisture. Then the samples were cut with a sterile blade along the longitude of the testis. Afterward, the tissue was gently pushed out, ensuring complete separation of the leukomalacia, and the "white thread" connecting the tissue was removed using Micro Forceps. Lastly, the tissue was carefully shaped into a chyme form.

The tissue chyme of one testis was mixed with 8 mL of IV collagenase (Gibco, Cat. NO.: 17104-019) at a concentration of 1 mg/mL in a 10 cm dish and subjected to digestion at 37 °C for 8-15 min. Throughout the digestion process, the tissue was gently pipetted and blown repeatedly. The mixture was subsequently centrifuged at 500 g for 5 min, followed by a single wash with DPBS and centrifuged at 500 g for 5 min again.

Tab. 1. Primer Information

Gene	primer sequence	Product length	Gene bank entry number
WT1	F: TGAGCGAAGGTTTTCTCGTT	166bp	NM_001001264.1
	R: GCTGAAGGGCTTTTCACTTG		
GATA4	F: CGACACCCTAATCTCGATATGTT	142bp	XM_013990297.2
	R: TCATCTTGTGGTAGAGGCCG		
GAPDH	F: TCGGAGTGAACGGATTTGGC	189bp	NM_001206359.1
	R: TGACAAGCTTCCCGTTCTCC		
MMP1	F: AAAACCCCGTTCAGCCAAGT	122bp	NM_001166229.1
	R: GCGCATGTAGAACCTGTCTT		
IL21R	F: AAGAAGTGGAACTACAGGCTCC	197bp	XM_021086442.1
	R: ATACAGGTCTTGCCAGGTGA		
LOC100526118	F: TCATGCTTTTGCCAATATGCCC	247bp	XM_003128792.4
	R: ACTCTGGTTTTCAGGGCCTTCAG		

"F": Forward primer, "R": Reverse primer.

Then, the sample was added with three times the volume of pre-cooled erythrocyte lysate (Solarbio, Cat. NO.: R1010) to remove the residues of the red blood cells and the mixture was mixed by gently blowing it. The mixture was then incubated at 4 °C for 15 min, followed by centrifugation at 500 g for 10 min until the tissue attained a white appearance, removed the lysate and the tissue was washed once with DPBS. The resulting precipitate was transferred to a 10 cm dish, and 8 mL of 0.05% trypsin (Gibco, Cat. NO.: 25200-056) was added. Subsequently, the sample was incubated at 37 °C for 10 min, and the digestion was terminated by adding 10% fetal bovine serum (FBS) (Gibco, Cat. NO.: 16000-044).

Cell purification and culture

The above-mentioned samples were filtered using a 70 μm cell strainer (FALCON, Cat. NO.: 352350) to remove debris. After filtering, the cells were collected by centrifugation at 300 g – 400 g for 5 min and then were incubated in a petri dish with DMEM/F12 complete culture medium (Gibco, Cat. NO.: 11320033) supplemented with 10% FBS (Gibco, Cat. NO.: 16000-044) and 1% PS for differential adherence purification. The petri dish was gently shaken to promote cell adherence, and the liquid above the cells was carefully removed. This purification process was repeated three times with the intervals of 15 min, 4 h, and overnight, respectively. The adherent cells were incubated at 37 °C in a 5% CO_2 incubator (Model 3111, Thermo, USA), and the media were changed every 2-3 days. The cells of second to third passages were used for the studies.

RT-PCR

The primers for WT1 and GATA4 were designed based on the mRNA sequences available on NCBI, utilizing NCBI Primer. The glyceraldehyde-3-phosphate dehydrogenase (GAPDH) served as the internal reference gene. The primer sequences were listed in Table 1, and they were synthesized by Shanghai Bioengineering Co. Total RNA was extracted using TRIzol reagent (Invitrogen, Cat. NO.: 15596026) and chloroform extraction. The concentration and purity of the total RNA were determined using a Nano-100 spectrophotometer (Allsheng, Hangzhou, China), ensuring optimal values with ratios of A260/A280 (2-2.2) and A260/A230 (1.8-2.2). For the reverse transcription, 1 μg of RNA was used and reverse transcription was carried out using the Reverse Transcription Kit (TaKaRa, Cat. NO.: RR047A) following the manufacturer's instructions.

For RT-PCR analysis, the reaction system consisted of 10 μL of Premix Taq (Takara, Cat. NO.: RR902), 0.5 μL of each upstream and downstream primers (working concentration: 10 μM), 2 μL of 3-fold diluted cDNA, and 7 μL of sterile water. The PCR process comprised an initial denaturation step at 95 °C for 5 min, followed by denaturation at 95 °C for 30 s, annealing at 60 °C for 30 s, and extension at 72 °C for 30 s. Thirty-four cycles were performed, and the PCR products were subjected to analysis by 1.5% agarose gel electrophoresis. Images were captured using a chemical imager (Model 5200, Shanghai Tanon Company, China).

Western blot

Cells were lysed using protein extraction reagents containing protease and phosphatase inhibitors (Thermo Scientific, Waltham, MA, USA). Total protein was extracted, and the protein concentration was determined using the BCA protein concentration assay kit (Beyotime, Cat. NO.: P0012S). Based on the protein concentration, the SDS-PAGE super-sampling buffer was added. Denaturation was carried out at 100 °C for 10 min using a 12.5% fast gel kit (YaMei, Cat. NO.: PG110). Electrophoresis was performed with a program of 90 V for 15 min followed by 170 V for 50 min. Once electrophoresis was completed, the proteins were transferred from the polyacrylamide gel to a polyvinylidene fluoride (PVDF) membrane using the wet transfer method at 200 mA for 2 h. The transferred proteins were then fixed to the membrane at a 5% concentration. Skimmed milk powder (BD-Pharmingen, Cat. NO.: 232100) was added and incubated at room temperature for 2 h. After cleaning the membrane with TBST solution, it was incubated with Anti-Wilms Tumor Protein antibody [CAN-R9(IHC)-56-2] (1:500, Cat. NO.: 89901, Abcam) and β-Actin (13E5) Rabbit mAb (1:1000, #4970, CST) at 4 °C, overnight on a shaker for membrane cutting and incubation. The incubated hybridization membranes were washed three times with a TBST solution for 10 min each, and then secondary antibodies (Anti-rabbit IgG, HRP-linked antibody, 1:3000, #7074 or Anti-mouse IgG, HRP-linked antibody, 1:3000, #7076) were added and incubated at room temperature for 50 min, the membranes were washed with TBST solution three times, developed using Super Signal™ West Atto Developer (Thermo, Cat. NO.: A38554), and the protein bands were observed on a Tanon-5200 Chemiluminescence Imaging System (Shanghai, China).

Indirect immunofluorescence staining

Indirect immunofluorescence was used to evaluate the purity of the isolated SCs. The second passages of SCs were cultured in the 24-well plates, when they reached 70% of confluence, the culture medium was discarded, and the cells were washed twice with DPBS for 5 s each time. Then, the cells were fixed with 4% paraformaldehyde (LEAGENE, Cat. NO.: DF0135) at 4 °C, for 15 min and washed three times with DPBS for 5 minutes each. Subsequently, the cells were incubated with 0.1% Triton X-100 (Sigma, Cat. NO.: 9036-19-5) for 15 min, and after WT1 antibody (1:50) on a shaker, at 4 °C, overnight. The next day, the cells was placed at room temperature for 15 min, the medium was discarded, rinsed with DPBS buffer three times, each time for 5 min and then, the second antibody (Goat anti-rabbit IgG(H+L)594

(1:1000, Cat. NO.:32740, Invitrogen) was added. The cells were kept at room temperature and shielded from light for 1 h. Then, they were washed with DPBS for 5 min time. The nuclei were subsequently stained with Hoechst33342 solution (Beyotime, Cat. NO.:C1028) for 10 min, followed by another round of washing with DPBS for 5 min. Finally, the cells were observed and photographed using a fluorescence microscope (BX51, Olympus, Japan).

CCK-8 for assessing cell viability

The passage 2 of SCs was resuscitated in culture medium in10 cm dishes and cultured for 2 days until they reached 80-90% of confluence. The cells were isolated and counted using a cell counter (Model FC610, Clinde, China). A total of 25,000 cells per well were then seeded into 96-well plates and incubated overnight. Then, the cells were treated with various concentrations of ZEA: 0, 5, 10, 15, 20, 25, 30, or 50 μM for 24 h. Then, each well was supplemented with 10 μL of CCK-8 reagent (Beyotime, Cat. NO.: C0038) and incubated for an additional 2 h at 37 °C. The absorbance at a wavelength of 450 nm was measured using a microplate reader (Molecular Devices, Spectra MaxM5, San Jose, CA, USA). The cell viability (%) was calculated using the following equation: (Absorbance of the experimental group - Absorbance of the blank) / (Absorbance of the control group - Absorbance of the blank) x 100%.

Detection of Intracellular ROS

Detection of ROS by immunofluorescence staining and flow cytometry

The ROS detection kit (Nan jing Jian cheng, Cat. NO.: E004-1) was utilized following the manufacturer's instructions. Briefly, the cell culture medium was discarded, and the cells were washed twice with DPBS. Then, the test group was treated with a serum-free culture medium containing a 10 μM DFCH-DA probe of 500 μL in each well in 12-well plate and incubated for 3 h. In the positive control group, the culture medium was supplemented with a serum-free culture medium containing a 10 μM DFCH-DA probe and 50 μg/mL of an active oxygen probe. The negative control group received a serum-free culture solution. After 2 h of incubation, the supernatant was discarded, and the cells were washed with DPBS four times. Subsequently, the nuclei were stained with Hoechst 33342 and incubated at 37 °C for 15 min. The cells were washed with DPBS three times, each for 5 min, and then imaged using fluorescence channels at 488 nm and 350 nm, respectively.

Following photography, the adherent cells were rinsed multiple times and subsequently transferred to 96-well plates. Each sample was replicated three times, and the fluorescence intensity was measured at 488 nm using a multifunctional fluorescence microscope (Spectra Max M5, Molecular Devices, USA). Part of the remaining cells were enumerated using a viable cell counter (FC610, Kolind, China) to determine the total cell count, which was then standardized. Another part of the remaining cells was used for flow cytometry analysis in which, the cell suspension was then passed through a 40 μm cell screen into the flow tube, and the FITC-A channel was selected. A FACSVerse flow cytometer (BD, Biosciences) was employed to analyze 10,000 cells. The experimental procedure was performed thrice to ensure reliability.

EdU assay for cell proliferation

Cell proliferation was assessed using the EdU assay kit (Biyun Tian, Cat. NO.:C0078S). Specifically, 1 mL of 10 μM EdU was added to cells in 12-well plates and incubated at 37 °C for 2.5 h. Subsequently, 500 μL of 4% paraformaldehyde was added and incubated at room temperature for 15 min. After removing the fixative solution, the cells were washed three times with 500 μL of 3% Bovine Serum Albumin (BSA) (SIGMA, Cat. NO.: A1933) for 5 min each. Then, the cells were incubated with 0.3% Triton X-100 permeabilizer at room temperature for 15 min. After a single wash, the click reaction solution was prepared according to the instructions. 250 μL of the reaction solution was added to each well of a 12-well plate and incubated at room temperature for 30 min, protected from light. The cells were then washed three times. The cell nuclei were stained using Hoechst 33342 and incubated at room temperature for 15 min. The cells were washed three times. Fluorescence microscopy was used to capture images in the 350 nm and 594 nm fluorescence channels.

ELISA for oxidative and antioxidant markers

Cells were collected by either digested with 0.25% trypsin or underwent cell scraping. The cells were then washed twice with DPBS and supplemented with 400 μL of pre-cooled DPBS. The mixture was placed on ice, and the cells were homogenized using an ultrasonic cell homogenizer (Sonics, USA, Model VCX130) The homogenate was centrifuged at 12000 rpm/min at 4 °C for 5 min. The supernatant was collected for the determination of T-AOC (Cat. NO.: A015-3-1), CAT (Cat. NO.: A007-1-1), GSH-PX (Cat. NO.: A005-1), and MDA (Cat. NO.: A003-4-1). Detailed operational instructions can be found in the Nan jing jian chen Reagent Kit manual.

RNA-seq and data analysis

Total RNA was extracted from 3 control, 3 ZEA-treated, and 3 ZEA+DBP2-treated swine SCs, respectively with the Trizol reagent (Invitrogen, Cat. NO.:15596026, USA). The concentration of RNA was quantified using a Qubit 4.0 (Thermo Scientific, USA), RNA quality was assessed using a Nano Drop spectrophotometer (TIANGEN, Cat. NO.: OSE-260-01), and RNA integrity was evaluated with an Agilent 2100 (Agilent Technologies, Santa Clara, CA, USA). RNA samples with a 260/280 ratio of approximately 2.0 were used in this analysis.

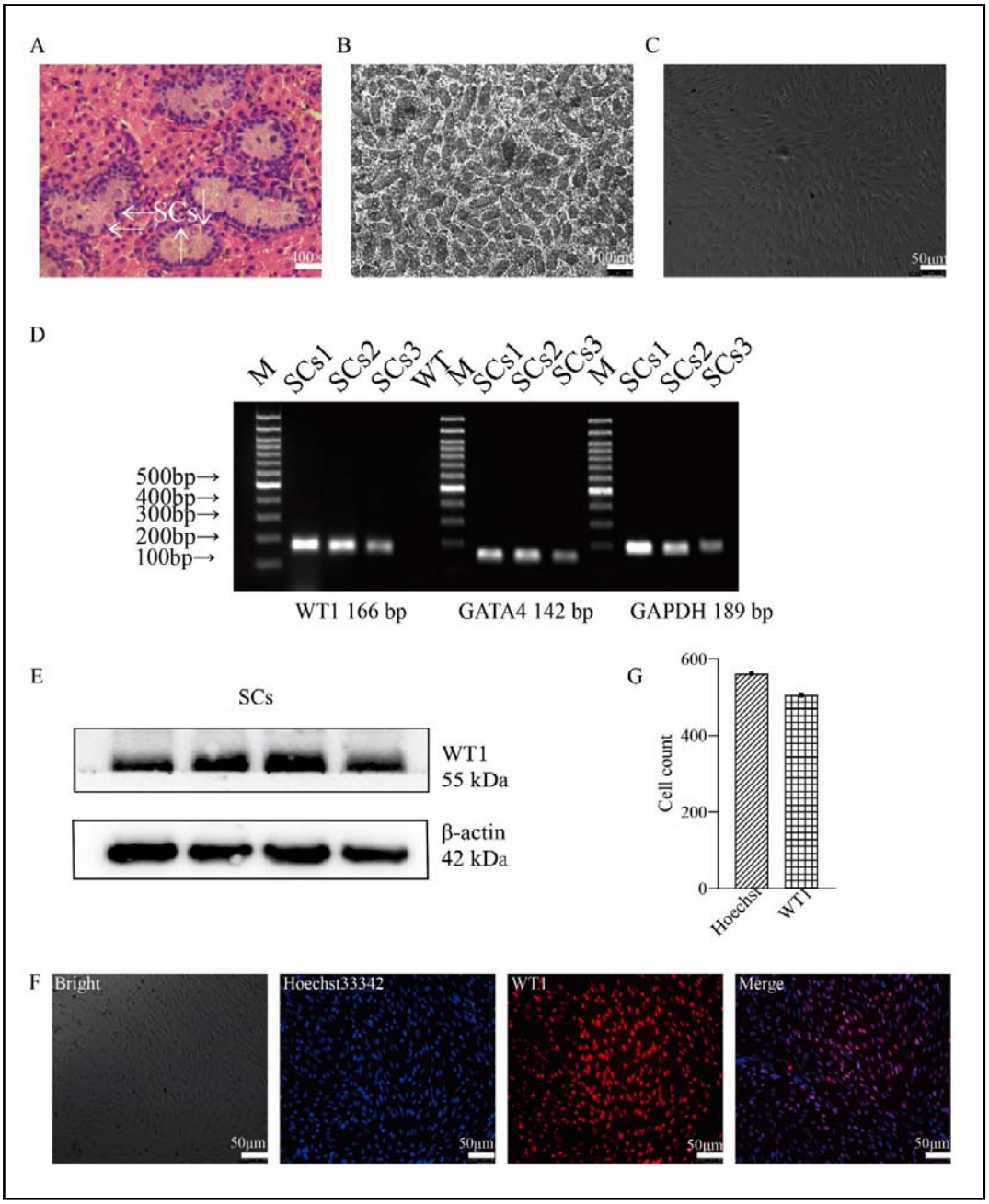

Fig. 1. Isolation and identification of swine SCs
(A) The swine testicular tissue at 7 days of age and the morphology of SCs by HE stains (400×), and the white arrowheads pointed to swine SCs. (B) Testicular tissue of the testis after collagenase digestion of the convoluted spermathecal tubules (scale bar = 100 μm). (C) SCs enriched by purification such as differential wall affixation (scale bar = 50 μm). (D-F) Isolated primary cells were identified, and SC marker genes were detected using RT-PCR, Western Blotting, and indirect immunofluorescence staining, respectively. (In D, M: markers, WT: water). (G) The purification efficiency was quantified using ImageJ analysis software, and the WT1 positive rate in F was 90% (506/562) (scale bar = 50 μm)

The libraries were prepared using the Hieff NGS® Ultima Dual-mode mRNA Library Prep Kit for Illumina® (Next Sage Biotech, Cat. NO.:12301, Shanghai, China) and sequenced on the DNB-seq T7 platform (Shenzhen Ji yin ga, Shenzhen, China) in a single lane. Following the removal of reads with low quality and adaptor contamination, the remaining reads were aligned to the swine genome (Sscrofa11.1) using the STAR2 alignment software. Detailed information regarding the generated short reads listed in Table S1. The transcripts were assembled by using StringTie (v1.3.2d), and the expression level of each gene was quantified using FPKM (Fragments Per Kilobase Million) (Fu *et al.* 2021).

DEGs were identified by using the DESeq (v1.16.0) package (http://www.bioconductor.org/packages/release/bioc/html/DESeq.html), based on the read count file obtained from (v0.6.0). A gene was considered significant if the Benjamini and Hochberg-adjusted P-value was less than 0.05 and the absolute log2 fold change was equal to or greater than 1.2. The identified DEGs underwent enrichment analysis by using Gene Ontology (GO) and KEGG (Kyoto Encyclopedia of Genes and Genomes) tools. The raw RNA-seq data have been deposited in NCBI GEO with the accession number SRP486547.

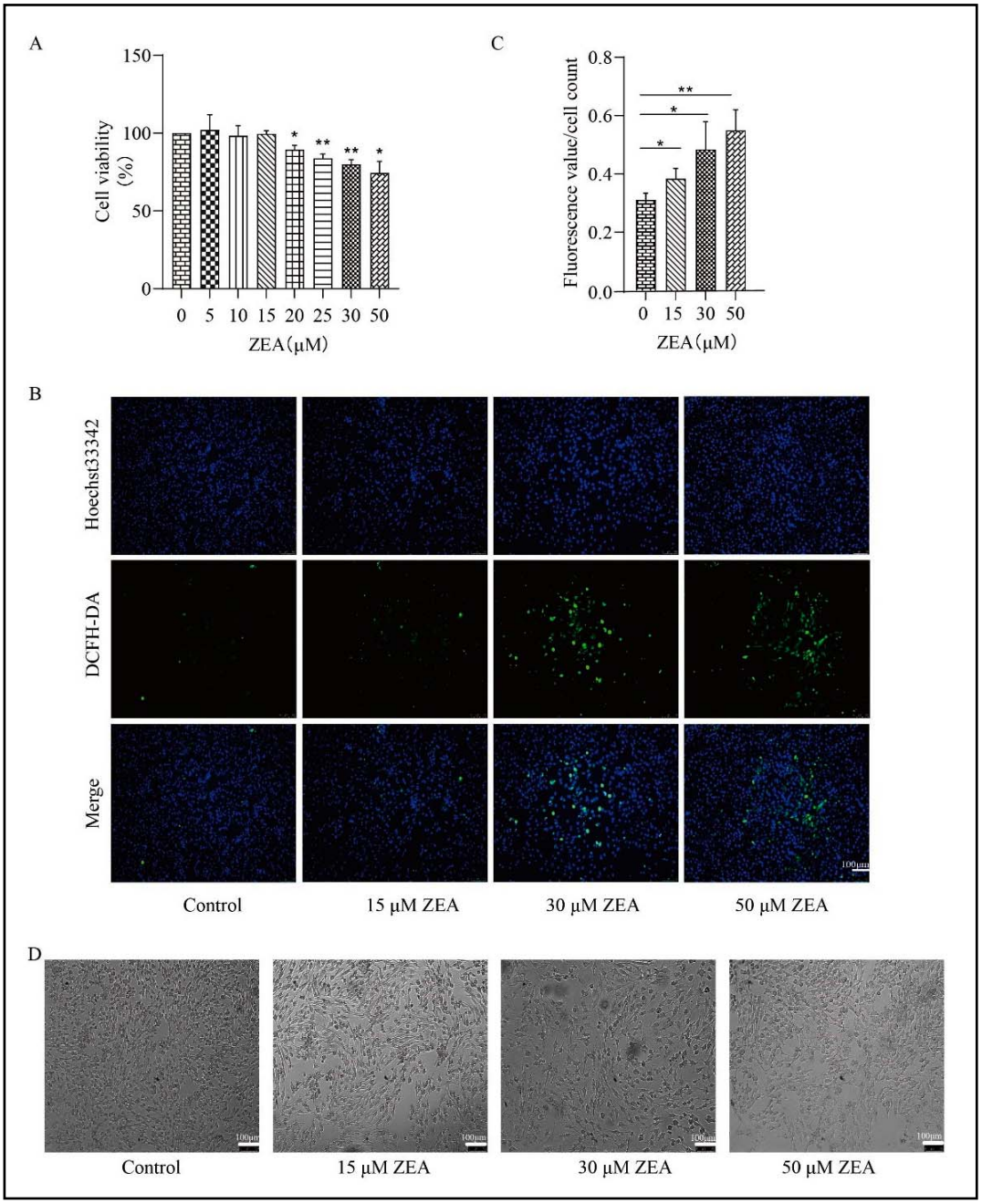

Fig. 2. Effects of ZEA at different concentration on 24 h of cultured swine SCs (A) Cell viability measured by CCK-8 assay. (B-C) The intracellular ROS levels detected by immunofluorescence assay (scale bar = 100 μm), (C) The fluorescence value using Microplate Reader. (D) The cell morphology (scale bar = 100 μm). Data from three independent experiments are expressed as mean ± SEM. * $p < 0.05$, ** $p < 0.01$, *** $p < 0.001$.

RT-qPCR validation of the DEGs

The cDNA extraction method was detailed in RT-PCR and the primer sequences listed in table 1. For RT-qPCR, a reaction system with a final volume of 20 μL consisted of 10 μL of 2× Real Star Fast SYBR qPCR Mix (Gen Star, Cat. NO.: A301), 1 μL of cDNA, 0.5 μL each of the upstream and downstream primers (at a working concentration of 10 μM), and 8 μL of sterile water. The PCR program consisted of an initial denaturation step at 95 °C for 2 min, followed by cycles of denaturation at 95 °C for 15 s, annealing at 60 °C for 30 s, and extension at 72 °C for 30 s, with a total of forty cycles. An ABI 7500 Rapid Real-Time Fluorescence Quantitative PCR System (Applied Biosystems, Waltham, MA, USA) was used for RT-qPCR. GAPDH served as the internal reference gene. The relative mRNA expression levels were determined by normalizing the gene expression to GAPDH using the $2^{-\Delta\Delta Ct}$ method. The primer sequences used for RT-qPCR listed in Table 1. The results were presented as fold change relative to the control.

Statistical Analysis

The fluorescence staining results and WB protein bands were quantified and merged using ImageJ 1.8.0 software. The ROS data measured by flow cytometry were analyzed using Flow Jo software, with FITC-A as the x-coordinate and Histogram as the y-coordinate. The RT-qPCR results were qualified by using GraphPad Prism 8.0 software, and the results were graphed. The

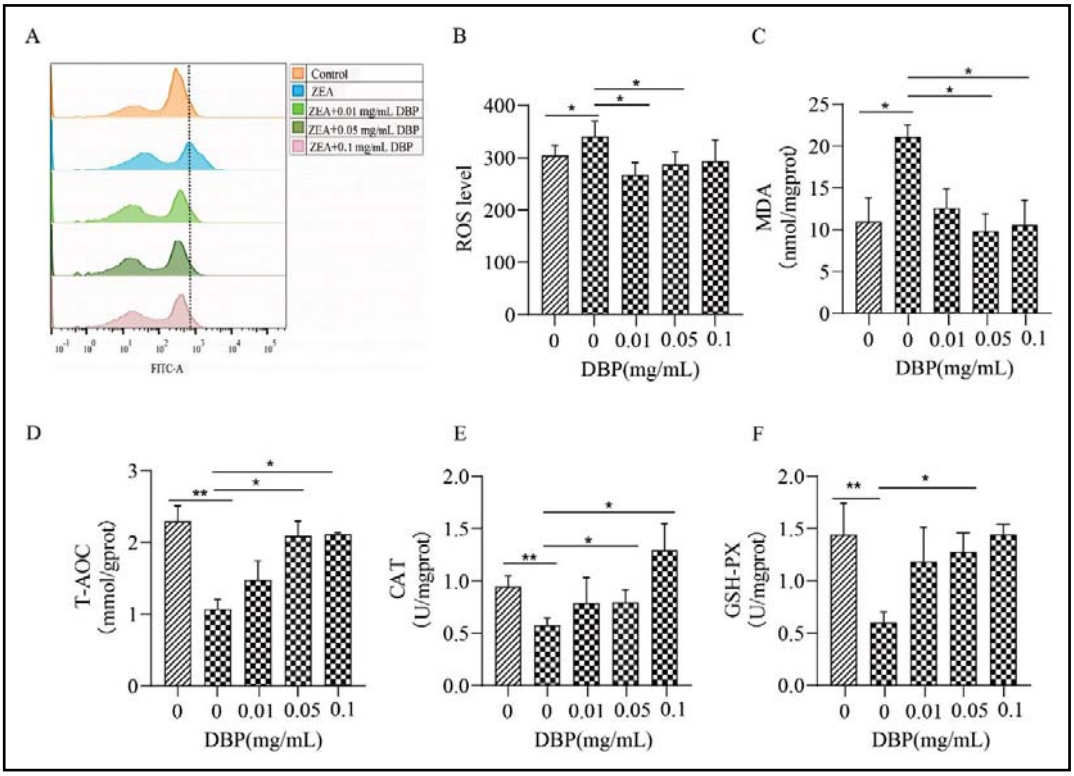

Fig. 3. Effects of DBP on ZEA induced oxidative damage in swine SCs (A) Intracellular ROS level assessed by flow cytometry. (B) The statistical analysis of data from A.(C) malondialdehyde (MDA) content. (D) T-AOC level. (E)catalase (CAT) activity. (F)GSH-PX activity. Data from three independent experiments are expressed as mean ± SEM. * $p < 0.05$, ** $p < 0.01$, *** $p < 0.001$.

data were presented as mean ± standard deviation. Comparisons between the two groups were evaluated with an unpaired t-test. Statistical significance was defined as $p < 0.05$ and denoted with an asterisk (*$p < 0.05$, **$p < 0.01$, ***$p < 0.001$). Each statistical analysis was conducted using at least three independent experiments.

RESULTS

Identification of the swine SCs with HE staining

Figure 1A illustrates the results obtained from HE stains of testicular tissues. The staining confirmed the cellular morphology and demonstrated that the testes of 7-day-old swine exhibited normal development. The testicular section showed the normal seminiferous tubules and the interstitial region. SCs, identified as columnar epithelial cells resembling irregular cones, were located on the basement membrane of the seminiferous tubules' walls. Their apical ends extended towards the luminal surface of the tubules. Notably, the swine SCs were surrounded by spermatogonia cells at various developmental stages, as indicated by the white arrows in the figure.

The characterization of cultured swine SCs

The seminiferous tubules of the testicular tissue after collagenase digestion were showed in Figure 1 B. The isolation and purification of swine SCs were made by the differential apposition method. The cultured swine SCs began to adhere after 15 min incubation and almost completed their adhesion at the following day. The results showed that at the lower cell density, SCs exhibited an elongated, willow-like shape and, at the high cell density, SCs had a shuttle-like morphology (Figure 1C). Semi-quantitative analysis confirmed the expression of swine testicular support cell-specific genes, Wilms tumor protein 1 (WT1), and zinc finger transcription factor GATA4 in the SCs (Figure 1D) and the protein-level expression of WT1 was also validated (Figure 1E) to further confirm that they were the genuine swine SCs.

Immunofluorescent staining demonstrated a 90% positivity rate for WT1 (Figure 1F-G). These findings corroborated the successful isolation and acquisition of swine SCs in our study.

Effects of ZEA treatment on cultured SCs

The results showed that the swine SCs treated with ZEA for 24 h significantly reduced the cell viability compared to the control with a dose-dependent manner ($p < 0.05$) (Figure 2A). This cell death was collaborated with significantly elevated intracellular levels of ROS compared to control and the increase of ROS also showed a dose-responsive manner ($p < 0.05$) (Figure 2B-C). ZEA treatment induced morphological changes in swine SCs, including a transition from a shuttle shape to an irregular shape and elongated filaments. Additionally, there was a decrease in cell number and increase in abnormal cells. (Figure 2D).

Effects of DBP on ZEA induced oxidative damage in SCs

All the studies were caried out for a period of 24 h incubation for both ZEA and DBP. ZEA treatment significantly increased the intracellular level of ROS measured

by the flow cytometry and DBP addition significantly suppressed this ROS increase caused by ZEA (Figure 3 A-B). ZEA treatment significantly reduced the T-AOC, CAT and GSH-PX activity but elevated the content of MDA compared to the control groups. However, DBP treatment at certain concentrations partially or completely reversed all these pathological alterations caused by ZEA ($p < 0.01$) (Figure 3 C-F). These results revealed that DBP enhanced cellular antioxidant capacity and mitigated ZEA induced oxidative damage in swine SCs, with the most protective effect of DBP being at a concentration of 0.05 mg/mL.

The effects of ZEA and DBP on gene expressions of swine SCs

Transcriptome sequencing was used to identify differentially expressed genes (DEGs) in SCs treated by ZEA or/and DBP. The significant differentiation was

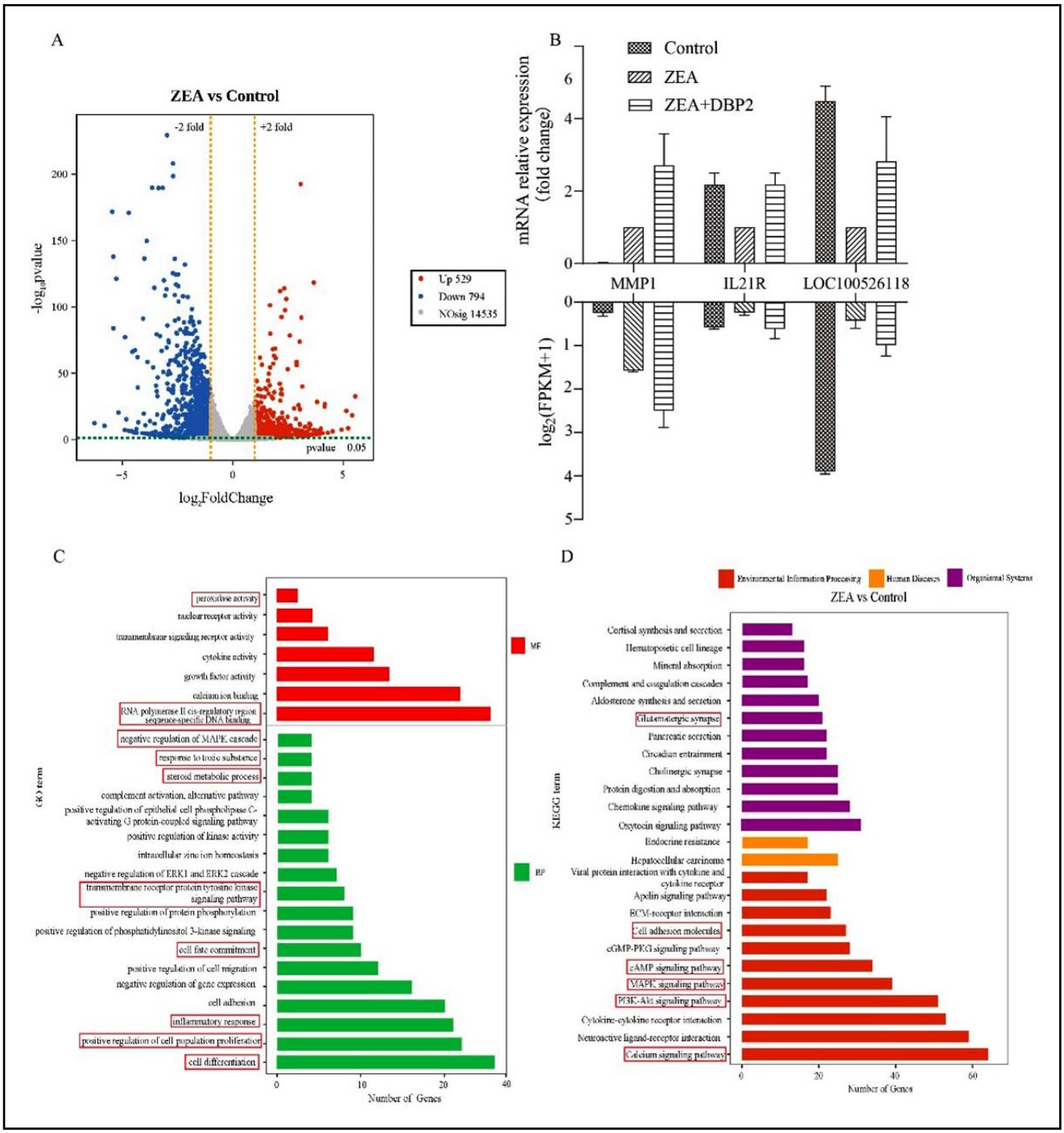

Fig. 4. The effects of ZEA on gene expressions of swine SCs (A) Volcano plot of 539 up-r and 794 down-regulated DEGs in ZEA-treated swine SCs relative to controls. (B) Validation of randomly selected DEGs by RT-qPCR. (C) GO function enrichment analysis shows correlation terms in the top 35 biological process (BP) and molecular function (MF) of all DEGs. (D) Enrichment analysis by KEGG pathway showing relevant terms in the top 35 pathways for all DEGs.

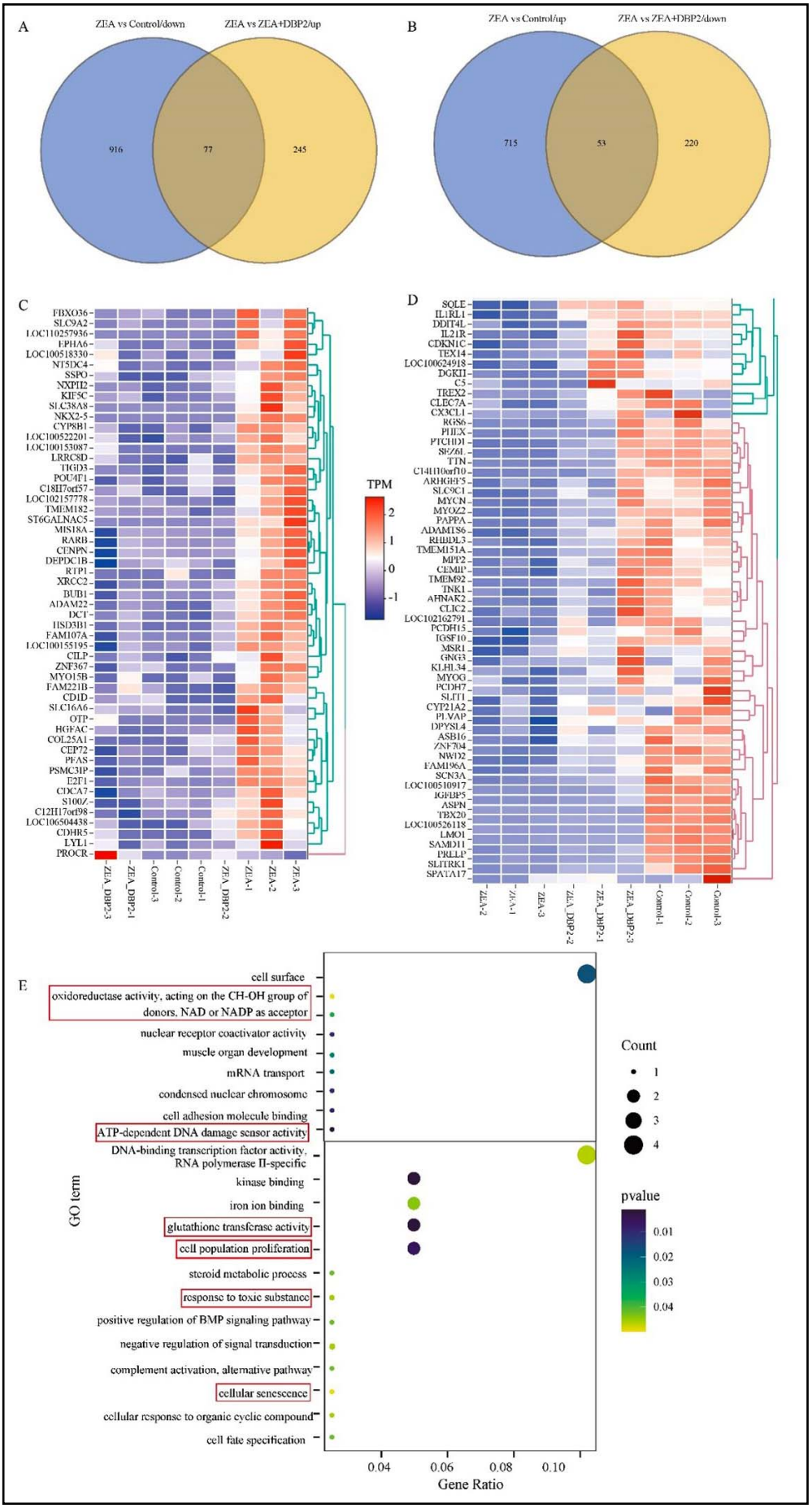

Fig. 5. The effects of ZEA plus DBP on gene expressions of swine SCs (A) Overlap between up-regulated genes in the control and ZEA groups and down-regulated genes in the ZEA and ZEA + DBP2 groups. (B) Overlap between down-regulated genes in control and ZEA groups and up-regulated genes in ZEA and ZEA + DBP2 groups. (C) Heat map of down-regulated genes with ZEA + DBP2 treatment. (D) Heatmap of up-regulated genes with ZEA + DBP2 treatment. (E) GO enrichment analysis of reversed genes after ZEA + DBP2 treatment.

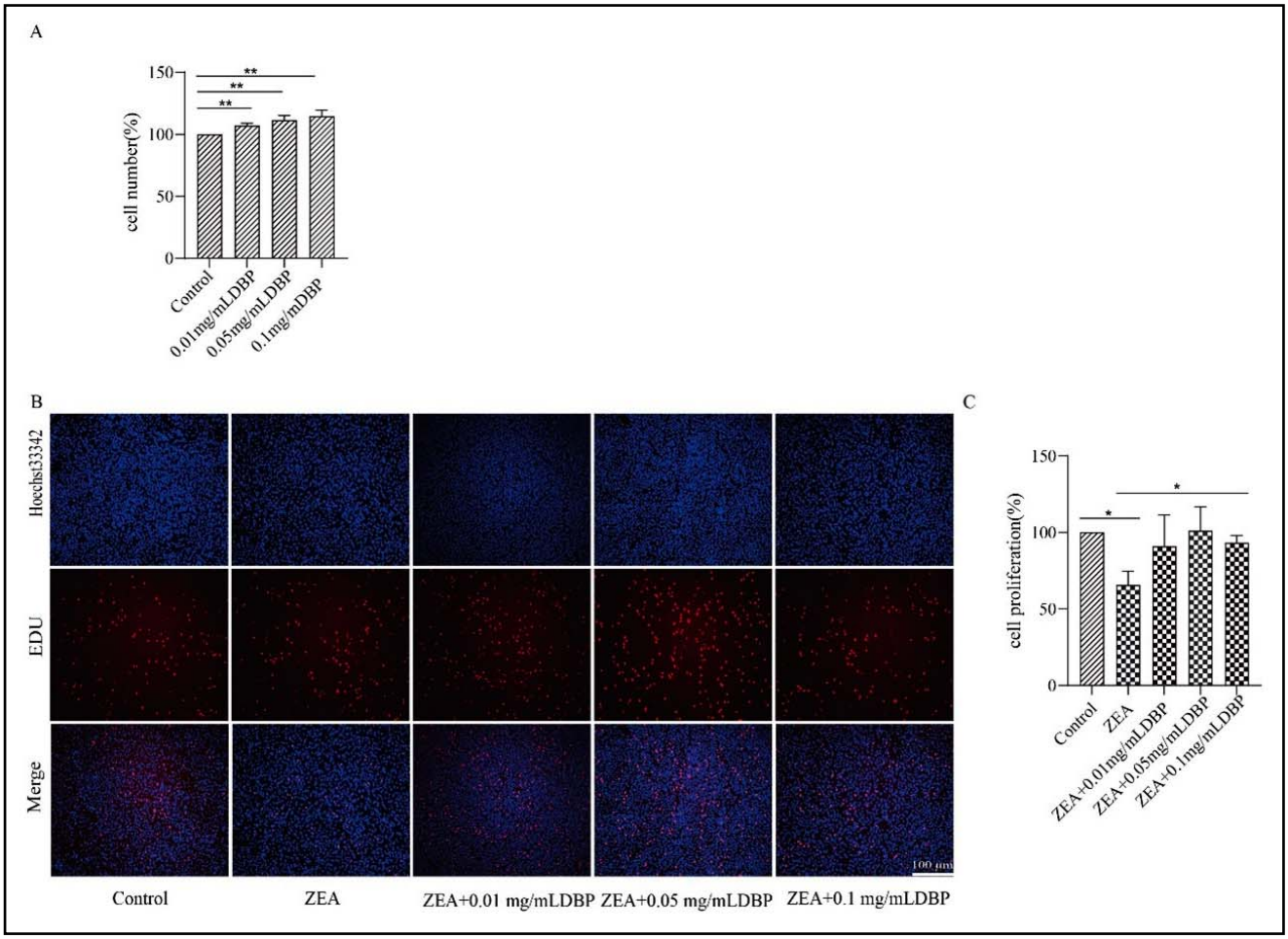

Fig. 6. Effects of ZEA and DBP on SCs proliferation (A) Effects of DBP on cell number compared to control. (B)The SCs EDU staining. (C) The statistical analysis of (B). N =3, * $p < 0.05$, ** $p < 0.01$

on set the cut of |log2fold change| ≥ 1 and a p value < 0.05 (Figure 4A). Statistical analysis revealed 1323 DEGs between the ZEA and control groups. Among them 529 genes were up- and 794 genes were down-regulated. These genes primarily involved cell growth, metabolism, peroxidase activity, and transcriptional regulatory activity (Table S1). To validate the results, three randomly selected DEGs (MMP1, IL21R, and LOC100526118) were verified by RT-qPCR and normalized using GAPDH as the internal reference gene. The results corroborated the trends observed in the sequencing data, confirming the reliability of the sequencing results (Figure 4B). The GO enrichment analysis of DEGs has identified a variety of biological processes, including cell differentiation, cell proliferation, inflammatory response, cell fate decision, toxicant response, negative regulation of MAPK cascade, steroid transmembrane signaling protein complex kinase signaling pathway, and other pathways (Figure 4C; Table S2). KEGG pathway analysis of DEGs revealed various signaling pathways of potential significance, such as glutamatergic synapses, cellular adhesion molecules, cAMP signaling pathway, MAPK signaling pathway, PI3K-Akt signaling pathway, calcium signaling pathway, and others (Figure 4D; Table S3).

Consistently, when DBP was added to the swine SCs culture medium, majority of the DEGs caused by ZEA were reversed with only 53 genes up- and 77 genes down-regulated (Figure 5A, B). Heat maps showed the gene clustering pattern that DBP plus ZEA treated group was more closely aligned with the control group than that of the ZEA treated alone, suggesting that DBP plays a role in restoring homeostasis on swine SCs. The GO analysis for all these genes (Figure 5C, D; Table S4), also showed the significant enrichment of terms related to cell proliferation, cellular senescence, toxicant response, glutathione transferase activity, and oxidoreductase activity (Figure 5E; Table S5).

Effects of ZEA and DBP on SCs proliferation

Based on the KEGG and GO analyses that the several signaling pathways related to the cell proliferation were enriched by DBP, therefore, the effects of DBP on SCs were investigated. First, the cell proliferation was evaluated by CCK-8 assay. The results showed that DBP appeared to significantly increase the swine SCs cell numbers in the cell culture with dose responsive

manner compared to the control group ($p < 0.01$) (Figure 6A), indicating an increased cell proliferation ($p < 0.05$) (Figure 6B). Then, cell proliferation was evaluated by EdU fluorescence staining which is more specifically to reflect the cell proliferation. The results showed that ZEA significantly suppressed swine SCs proliferation indicated by the reduced EdU fluorescence staining compared to the control group while the addition of DBP2 reversed this suppression and increased swine SCs proliferation comparable to both ZEA and control group.

DISCUSSION

A successful swine breading greatly depends on the quality of the sperms. The spermatogenesis requires the functional SCs which form a blood-testis barrier for protection and provide structural and nutritional supports for spermatogenic cell development (Cao *et al.* 2021). However, SCs of swine are more vulnerable to the environmental insults than other species. For example, the environmental toxin ZEA can cause swine SCs oxidative damage and jeopardizes the quality of the sperms. It seems that to increase the antioxidative capacity of the SCs is a suitable strategy to improve the quality of sperms. Several studies have confirmed the beneficial effects of this strategy for swine spermatogenesis (Liu *et al.* 2022a). Based on the best of our knowledge, DBP, a naturally occurring novel antioxidant, has not been tested its protective effects on swine reproductive system, particularly on SCs. In the current study, the potential protective effects of DBP on the ZEA induced oxidative damage in swine SCs have been systemically investigated.

The reproductive toxicity of ZEA has been reported in variety of species and different cells including goat Sertoli cells, swine granulosa cells, swine testicular cells (Liu *et al.* 2023), bovine mammary epithelial cells (Fu *et al.* 2021), and IPEC-J2 cells (Sun *et al.* 2021), suggesting that its toxic effects are across the species. The major underline mechanism is that ZEA and its metabolite promote the reactive oxygen species (ROS) formation and subsequently to trigger autophagy (Bai *et al.* 2023), senescence (Wang *et al.* 2023a), and oxidative damage (Skrzydlewski *et al.* 2022) of related cells. Our results confirmed that ZEA also caused swine SCs oxidative damage indicated by the increased intracellular ROS and MDA content, the decreased T-AOC, CAT, GSH-PX activities as well as the reduced survival rate of SCs. In the in vivo study, it has been reported the ZEA decreases in the number of spermatogenic cell layers within swine testicular tissues resulted in reduced fertility (Liu *et al.* 2022).

In the current study, the DBP was selected to protect against the ZEA induced SCs oxidative damage. This selection is based on the potent antioxidative capacity of DBP and the beneficial effects of other similar products on oxidative tissue damage. For example, in A mice study, the phospholipids of soy lecithin combined with soy isoflavones prevented beta-amyloid (Aβ) -induced cognitive deficits by regulating abnormal cerebral blood flow by protecting antioxidant activity in brain vessels (Li *et al.* 2023). In addition, it was found that the accumulation of Aβ in the brain might relate to the degradation of ethanolamine acetal phosphatidylcholine hydroperoxide substances and increased levels of phosphatidylcholine hydroperoxide in the blood of Alzheimer's patients (Yamashita *et al.* 2016), as well as an increased general marker of lipid peroxidation (Ademowo *et al.* 2017). Deoiled soy lecithin has antioxidant property, and its supplementation reversed the low metabolic energy diet induced growth retardation in Turkeys and reduced their serum triglycerides, total cholesterol, and MDA, and increased their serum superoxide dismutase activity (Nemati *et al.* 2021). The combination of lecithin and ascorbic acid reduced the mechanical fragility and hemolysis of red blood cells, and increased the deformability, which suggested its use in preparing long-term anti-hemolysis blood-contact biomaterials (Shi *et al.* 2015). Various phospholipids extracted from rapeseed (Aleman *et al.* 2021), walnuts (Martinez *et al.* 2010), etc., also have antioxidant activities. Our results showed the profound protective effects of DBP on ZEA induced oxidative damage in SCs. DBP supplementation significantly lowered the intracellular ROS level and restored the T-AOC and the disturbed antioxidant enzyme activities. Since DBP is a relatively new brand of antioxidant, the molecular mechanisms as to how the DBP promotes the antioxidative enzymes including CAT and GSH-PX is currently unknown and to identify them is the goal of our future studies.

In the study, we also noticed that DBP not only reduced the SCs cell death caused by the ZEA but also improved the SCs proliferation. These findings align with a previous study in which it showed that antler blood extract promoted cell proliferation at wound sites (Ma *et al.* 2024).

To explore the underline mechanisms, the transcriptome sequencing analysis was performed. The combined results of DEGs, GO and KEGG enrichment analyses showed that DBP treatment involved various signaling pathways of potentially biological significance including MAPK signaling and PI3K-Akt signaling pathways.

MAPK signaling pathway involves in a myriad of extracellular and intracellular stress responses (Stefani *et al.* 2021; Wang *et al.* 2023c). This pathway is critical in regulating various cellular functions, including proliferation, survival, growth, transcription, and protein synthesis (Lin *et al.* 2022). It often collaborates with the P38 signaling pathway to regulate the cell cycle, apoptosis, or senescence (García-Flores *et al.* 2023). Inhibition of p38 phosphorylation by MAPK was observed to modulate the cell cycle. Consequently, significant downregulation of it alleviated neuronal cell death occurred in cadmium induced Sertoli cell injury

(Chen *et al.* 2023; Wang *et al.* 2023b). In addition, PI3K/AKT signaling pathway is crucial in coordinating intracellular signaling in response to extracellular stimuli to promote cell proliferation such as in tumor cells (Noorolyai *et al.* 2019). These data suggest that the effects of DBP on SCs proliferation may be mediated by the MAPK/ PI3K/AKT signaling pathways.

Based on the results mentioned above, the cell proliferation was re-evaluated by CCK-8 and EdU fluorescence staining which is the biomarker of cell proliferation. CCK-8 assay showed DBP treatment significantly increased the cell number compared to the control group and this result indirectly indicated the proliferation promoting effects of DBP. In EdU fluorescence staining study, the DBP significantly increased the EdU fluorescence staining in SCs compared to both control and ZEA treated groups. The EdU fluorescence staining result directly confirmed that DBP indeed, promoted cell proliferation.

CONCLUSION

In conclusion, we have, for the first time reported that a naturally occurring novel antioxidant DBP has the capacity to protect against ZEA induced oxidative damage in the cultured swine SCs. The results suggest that the potential mechanisms are mediated by its action on the enhancement of intracellular antioxidative enzymes' activities and reduction of ROS. In addition, it also can enrich the MAPK as well as PI3K/AKT signaling pathways to promote SCs proliferation. Its effects will be test in vivo in the future. If confirmed, DBP will be considered as a suitable candidate to find its use in improvement of male swine reproductive activity.

CONFLICT OF INTEREST

The authors declare no conflict of interest.

ACKNOWLEDGMENT

The authors would like to thank all the participants for their time. Special thanks to Dr. Dunxian Tan and Dr. Ximing Guo for their comments and suggestions on the manuscript.

FUNDING

This research was funded by the National Natural Science Foundation of China, grant number 32172738; School start-up plan, Project number XYB201911.

REFERENCES

1 Abah KO, Fontbonne A, Partyka A, Nizanski W. (2023). Effect of male age on semen quality in domestic animals: potential for advanced functional and translational research? Vet Res Commun **47**: 1125-1137.

2 Ademowo OS, Dias HKI, Milic I, Devitt A, Moran R, Mulcahy R, et al. (2017). Phospholipid oxidation and carotenoid supplementation in Alzheimer's disease patients. Free Radic Biol Med **108**: 77-85.

3 Chen X, Ning Y, Wang B, Qin J, Li C, Gao R,et al. (2023). HET0016 inhibits neuronal pyroptosis in the immature brain post-TBI via the p38 MAPK signaling pathway. Neuropharmacology **239**: 109687.

4 Cimbalo A, Frangiamone M, Font G, Manyes L. (2022). The importance of transcriptomics and proteomics for studying molecular mechanisms of mycotoxin exposure: A review. Food Chem Toxicol **169**: 113396.

5 Fu Y, Jin Y, Shan A, Zhang J, Tang H, Shen J, et al. (2021). Polydatin Protects Bovine Mammary Epithelial Cells Against Zearalenone-Induced Apoptosis By Inhibiting Oxidative Responses and Endoplasmic Reticulum Stress. Toxins (Basel) **13**: 121.

6 Gajęcka M, Rybarczyk L, Zwierzchowski W, Jakimiuk E, Zielonka L, Obremski K, et al. (2011). The effect of experimental, long-term exposure to low-dose zearalenone mycotoxicosis on the histological condition of ovaries in sexually immature gilts. Theriogenology **75**: 1085-1094.

7 Gao Y, Mruk DD, Cheng CY. (2015). Sertoli cells are the target of environmental toxicants in the testis - a mechanistic and therapeutic insight. Expert Opin Ther Targets **19**: 1073-1090.

8 García-Flores N, Jiménez-Suárez J, Garnés-García C, Fernández-Aroca DM, Sabater S, Andrés I, et al. (2023). P38 MAPK and Radiotherapy: Foes or Friends? Cancers (Basel) **15**: 861.

9 He J. (2022). The research on extraction and antioxidant activity of deer blood phospholipid and its application as drug carrier [dissertation]. China (Harbin): Harbin Institute of Technology.

10 Guo XM, Han HS, He J. (2022). A method for extracting phospholipid from deer blood and its application. China patent, Application No. CN 115043872A.

11 Kiseleva M, Chalyy Z, Sedova I, Aksenov I. (2020). Stability of Mycotoxins in Individual Stock and Multi-Analyte Standard Solutions. Toxins (Basel) **12**: 94.

12 Kuiper GG, Lemmen JG, Carlsson B, Corton JC, Safe SH, van der Saag PT, van der Burg B, Gustafsson JA. (1998). Interaction of estrogenic chemicals and phytoestrogens with estrogen receptor beta. Endocrinology **139**: 4252-4263.

13 Li H, Wang X, Li X, Zhou X, Wang X, Li T, Xiao R, Xi Y. (2023). Role of soy lecithin combined with soy isoflavone on cerebral blood flow in rats of cognitive impairment and the primary screening of its optimum combination. Nutr Res Pract **17**: 371-385.

14 Li L, Zhang T, Ren X, Li B, Wang S. (2021). Male reproductive toxicity of zearalenone-meta-analysis with mechanism review. Ecotoxicol Environ Saf **221**: 112457.

15 Li Y, Zhang B, Huang K, He X, Luo Y, Liang R, Luo H, Shen XL, Xu W. (2014). Mitochondrial proteomic analysis reveals the molecular mechanisms underlying reproductive toxicity of zearalenone in MLTC-1 cells. Toxicology **324**: 55-67.

16 Lin X, Zhu L, Gao X, Kong L, Huang Y, Zhao H, et al. (2022). Ameliorative effect of betulinic acid against zearalenone exposure triggers testicular dysfunction and oxidative stress in mice via p38/ERK MAPK inhibition and Nrf2-mediated antioxidant defense activation. Ecotoxicol Environ Saf **238**: 113561.

17 Liu J, Yao T, Weng X, Yao R, Li W, Xie L, Yue X, Li F. (2022). Antioxidant properties and transcriptome of cauda epididymis with different levels of fertility in Hu lambs. Theriogenology 182:85-95.

18 Liu H, Xue J, Li L, Mo H. (2022a). Shenjing Guben Wan promotes sperm development by increasing the activity of seminiferous epithelium Sertoli cells. Transl Androl Urol **11**: 867-876.

19 Liu X, Xi H, Han S, Zhang H, Hu J. (2023). Zearalenone induces oxidative stress and autophagy in goat Sertoli cells. Ecotoxicol Environ Saf **252**: 114571.

20 Mellagi APG, Will KJ, Quirino M, Bustamante-Filho IC, Ulguim RDR, Bortolozzo FP. (2023). Update on artificial insemination: Semen, techniques, and sow fertility. Mol Reprod Dev **90**: 601-611.

21 Minervini F, Dell'Aquila ME, Maritato F, Minoia P, Visconti A. (2001). Toxic effects of the mycotoxin zearalenone and its derivatives on in vitro maturation of bovine oocytes and 17 beta-estradiol levels in mural granulosa cell cultures. Toxicol In Vitro **15**: 489-495.

22 Nemati M, Ghasemi HA, Hajkhodadadi I, Moradi MH. (2021). De-oiled soy lecithin positively influenced growth performance, nutrient digestibility, histological intestinal alteration, and antioxidant status in turkeys fed with low energy diets. Br Poult Sci **62**: 858-867.

23 Nguyen ND, Le MT, Dang HNT, Van Nguyen T, Nguyen QHV, Cao TN. (2023). Impact of semen oxidative stress on sperm quality: initial results from Vietnam. J Int Med Res 51:3000605231188655.

24 Noorolyai S, Shajari N, Baghbani E, Sadreddini S, Baradaran B. (2019). The relation between PI3K/AKT signalling pathway and cancer. Gene **698**:120-128.

25 Qin X, Cao M, Lai F, Yang F, Ge W, Zhang X, et al. (2015). Oxidative stress induced by zearalenone in porcine granulosa cells and its rescue by curcumin in vitro. PLoS One **10**: e0127551.

26 Sengupta P, Roychoudhury S, Nath M, Dutta S. (2022). Oxidative Stress and Idiopathic Male Infertility. Adv Exp Med Biol **1358**: 181-204.

27 Sforza S, Dall'asta C, Marchelli R. (2006). Recent advances in mycotoxin determination in food and feed by hyphenated chromatographic techniques/mass spectrometry. Mass Spectrom Rev **25**: 54-76.

28 Shi Q, Fan Q, Ye W, Hou J, Wong SC, Xu X, et al. (2015). Binary release of ascorbic acid and lecithin from core-shell nanofibers on blood-contacting surface for reducing long-term hemolysis of erythrocyte. Colloids Surf B Biointerfaces **125**: 28-33.

29 Skrzydlewski P, Twarużek M, Grajewski J. (2022). Cytotoxicity of Mycotoxins and Their Combinations on Different Cell Lines: A Review. Toxins (Basel) **14**: 244.

30 Soffa DR, Stewart JW, Pack ED, Arneson AG, De Vita R, Knight JW, et al. (2023). Short-term consumption of the mycotoxin zearalenone by pubertal gilts causes persistent changes in the histoarchitecture of reproductive tissues. J Anim Sci **101**: skac421.

31 Stefani C, Miricescu D, Stanescu S II, Nica RI, Greabu M, Totan AR, et al. (2021). Growth Factors, PI3K/AKT/mTOR and MAPK Signaling Pathways in Colorectal Cancer Pathogenesis: Where Are We Now? Int J Mol Sci **22**: 10260.

32 Sun H, Xiao D, Liu W, Li X, Lin Z, Li Y, et al. (2024). Well-known polypeptides of deer antler velvet with key actives: modern pharmacological advances. Naunyn Schmiedebergs Arch Pharmacol **397**: 15-31.

33 Sun H, Zhang M, Li J, Shan A. (2021). DL-Selenomethionine Alleviates Oxidative Stress Induced by Zearalenone via Nrf2/Keap1 Signaling Pathway in IPEC-J2 Cells. Toxins (Basel) **13**: 557.

34 Sun Y, Huang K, Long M, Yang S, Zhang Y. (2022). An update on immunotoxicity and mechanisms of action of six environmental mycotoxins. Food Chem Toxicol **163**: 112895.

35 Tsakmakidis IA, Lymberopoulos AG, Alexopoulos C, Boscos CM, Kyriakis SC. (2006). In vitro effect of zearalenone and alpha-zearalenol on boar sperm characteristics and acrosome reaction. Reproduction in Domestic Animals **41**: 394-401.

36 Vicenova M, Nechvatalova K, Chlebova K, Kucerova Z, Leva L, Stepanova H, et al. (2014). Evaluation of in vitro and in vivo anti-inflammatory activity of biologically active phospholipids with anti-neoplastic potential in porcine model. BMC Complement Altern Med **14**: 339.

37 Wang K, Zhou M, Du Y, Li P, Huang Z. (2023a). Zearalenone induces the senescence of cardiovascular cells in vitro and in vivo. Environ Sci Pollut Res Int **30**: 56037-56053.

38 Wang L, Li X, Bu T, Wu X, Li L, Gao S, et al. (2023b). Cadmium-induced Sertoli Cell Injury Through p38-MAPK and Related Signaling Proteins-A Study by RNA Sequencing. Endocrinology **164**: bqad045.

39 Wang X, Tan X, Zhang J, Wu J, Shi H. (2023c). The emerging roles of MAPK-AMPK in ferroptosis regulatory network. Cell Commun Signal **21**: 200.

40 Wilson PR, Pauli JV. (1983). Blood constituents of farmed red deer (Cervus elaphus). II: biochemical values. N Z Vet J **31**: 1-3.

41 Yamashita S, Kiko T, Fujiwara H, Hashimoto M, Nakagawa K, Kinoshita M, et al. (2016). Alterations in the Levels of Amyloid-β, Phospholipid Hydroperoxide, and Plasmalogen in the Blood of Patients with Alzheimer's Disease: Possible Interactions between Amyloid-β and These Lipids. J Alzheimers Dis **50**: 527-537.

42 Yan WK, Liu YN, Song SS, Kang JW, Zhang Y, Lu L, et al. (2022b). Zearalenone affects the growth of endometriosis via estrogen signaling and inflammatory pathways. Ecotoxicol Environ Saf **241**: 113826.

43 Yang JH, Cao Y, Wang RL, Fei YR, Zhang H, Feng P, Liu J. (2010). Anti-resorptive effect of pilose antler blood (Cervus nippon Temminck) in ovariectomized rats. Indian J Exp Biol **48**: 554-558.

44 Yin M, Matsuoka R, Xi Y, Wang X. (2021). Comparison of Egg Yolk and Soybean Phospholipids on Hepatic Fatty Acid Profile and Liver Protection in Rats Fed a High-Fructose Diet. Foods **10**: 1569.

45 Zhao Z, Xu Y. (2010). An extremely simple method for extraction of lysophospholipids and phospholipids from blood samples. J Lipid Res **51**: 652-659.

46 Zinedine A, Soriano JM, Moltó JC, Mañes J. (2007). Review on the toxicity, occurrence, metabolism, detoxification, regulations and intake of zearalenone: an oestrogenic mycotoxin. Food Chem Toxicol **45**: 1-18